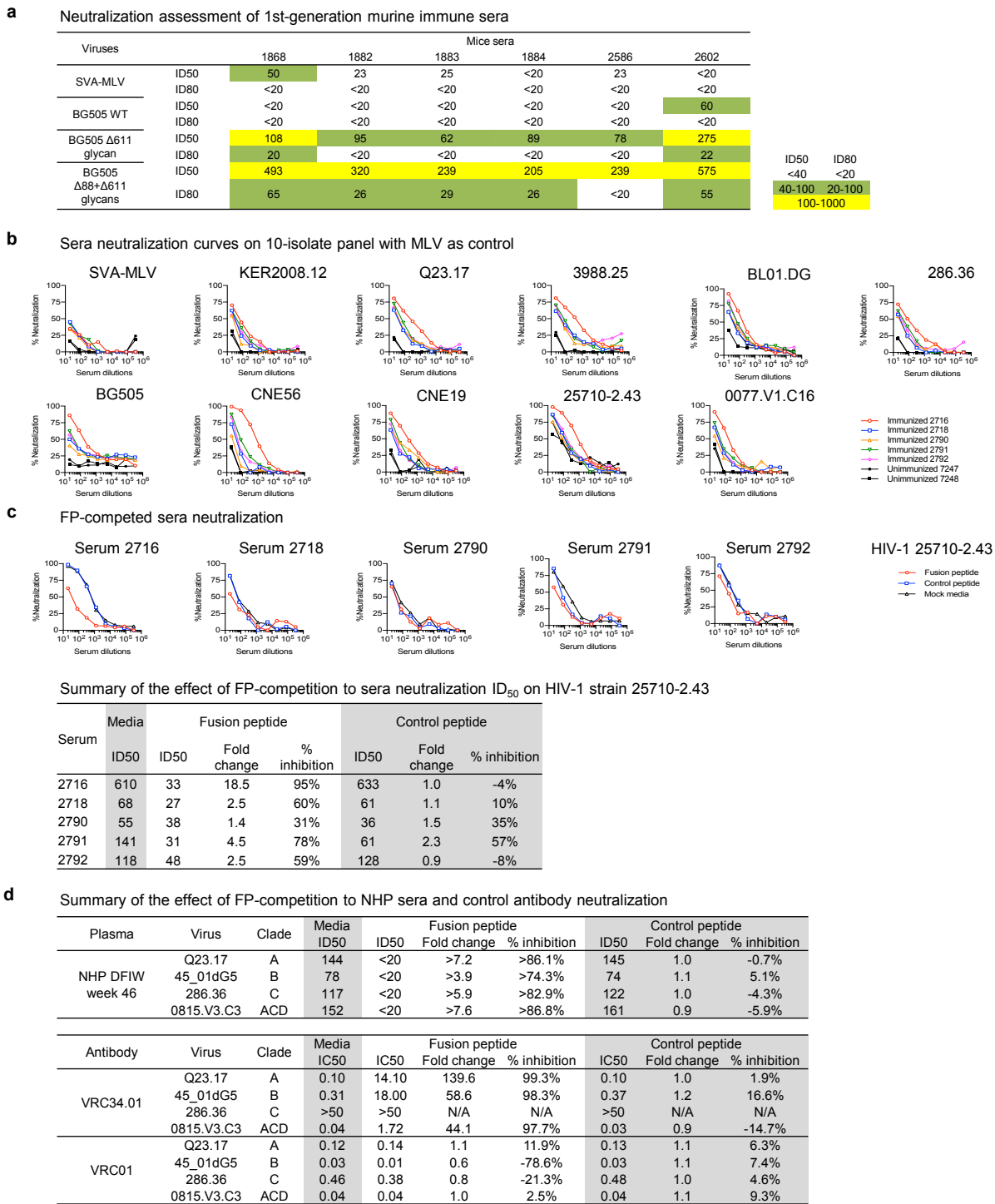


Supplementary Figure 1. Characteristics of FP immunogens. **a**, Metric of antigenicity. Here we focus on the FP site of vulnerability ($N=1$). VRC34.01, VRC34.05, PGT151, and ACS202 were used as the representative neutralizing antibodies targeting FP, and CH07 was used as the representative poorly/non-neutralizing antibody targeting FP. See (c) for K_D data. **b**, Antigenicity assessment of FP immunogens by BLI method with Octet. Examples of Octet-binding curves for FP8-KLH and FP-1M6T epitope scaffold are shown. **c**, FP-immunogen antigenicity. FP-directed antibodies VRC34.01, VRC34.02, PGT151 and ACS202 were considered neutralizing, whereas CH07 was considered weakly or non-neutralizing. **d**, Immunogen quality control by MSD. **e**, Amino acid sequences for FP scaffolds: FP-3SH and FP-1SLF. Additional epitope scaffolds are described in Kong et al. 2016. **f**, Structural models of FP-3SH and FP-1SLF. **g**, Negative-stain EM images (inset shows 2D-class averages). **h**, Physical stability of FP8-KLH. Fractional values refer to VRC34.01 reactivity retained after exposure to various physical extremes as compared to initial reactivity with VRC34.01. Affinity measured by biolayer interferometry. **i**, Binding of VRC34.01 Fab to FP8-KLH illustrated by negative-stain electron microscopy. Examples of micrographs for FP8-KLH (left) and FP8-KLH mixed with VRC34.01 Fab at a molar ratio of 1:10 (right). Right insets, examples of raw particles for FP8-KLH and FP8-KLH in complex with VRC34.01 Fab. White arrows indicate bound Fab fragments. Bottom insets, examples of 2D-class averages. White arrows indicate bound Fab fragments. For (b, f, g and i), $n=3$ experiments were performed independent with similar results.



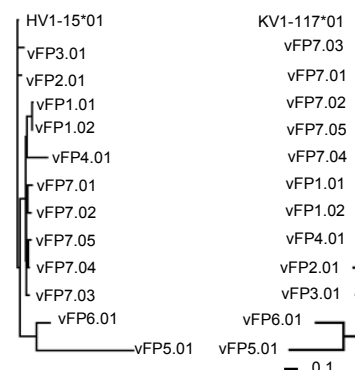
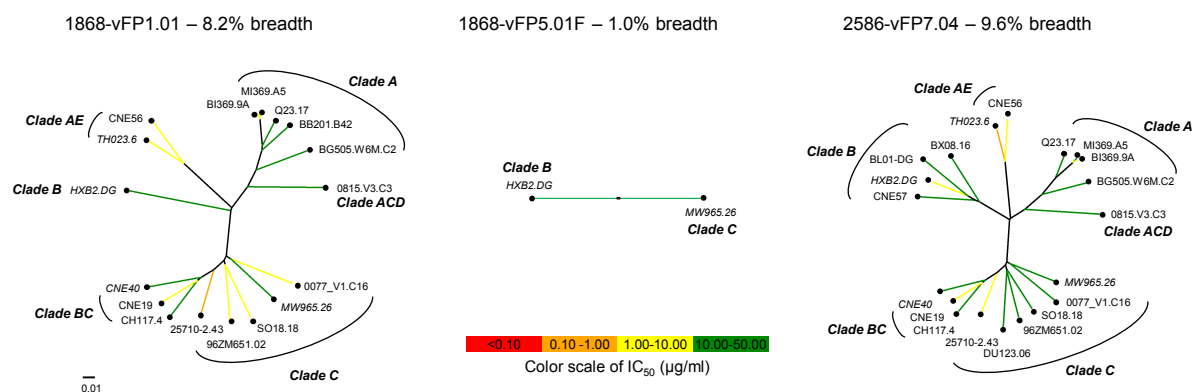
Supplementary Figure 2. Neutralization of immunized sera on 293T-derived HIV-1 Env-pseudotyped viruses in TZM-bl assay. **a**, Neutralization assessment of 1st-generation immune sera from immunized mice in Fig. 1. **b**, Neutralization assessment of 2nd-generation immune sera from immunized mice in Fig. 3c. Serum neutralization curves are shown for 5 immunized and 2 unimmunized control C57/BL6 mice, tested on 10 wildtype HIV-1 Env-pseudotyped viruses (5 with complete glycans around the FP site and 5 naturally missing glycans as shown in Fig. 3c along with ID₅₀ titer). SVA-MLV was assessed as a control. **c**, FP-competed neutralization curves of indicated immunized mice sera on HIV-1 strain 25710-2.43. Sera were pre-incubated with the nine-amino acid FP (sequence AVGIGAVFL) (red), a non-cognate FLAG peptide (blue) or control media (black) before mixing with virus stock. ID₅₀ titers are shown the summary table. ID₅₀ fold change was calculated as ID50[media]/ID50[peptide]. % inhibition of FP or control peptide was calculated as (1-ID50[peptide]/ID50[media])*100. **d**, Neutralization summary for FP competition shown in Fig. 6b. For antibody neutralization, IC50 fold change was calculated as IC50[peptide]/IC50[media]. % inhibition of FP or control peptide was calculated as (1-IC50[media]/IC50[peptide])*100.

a

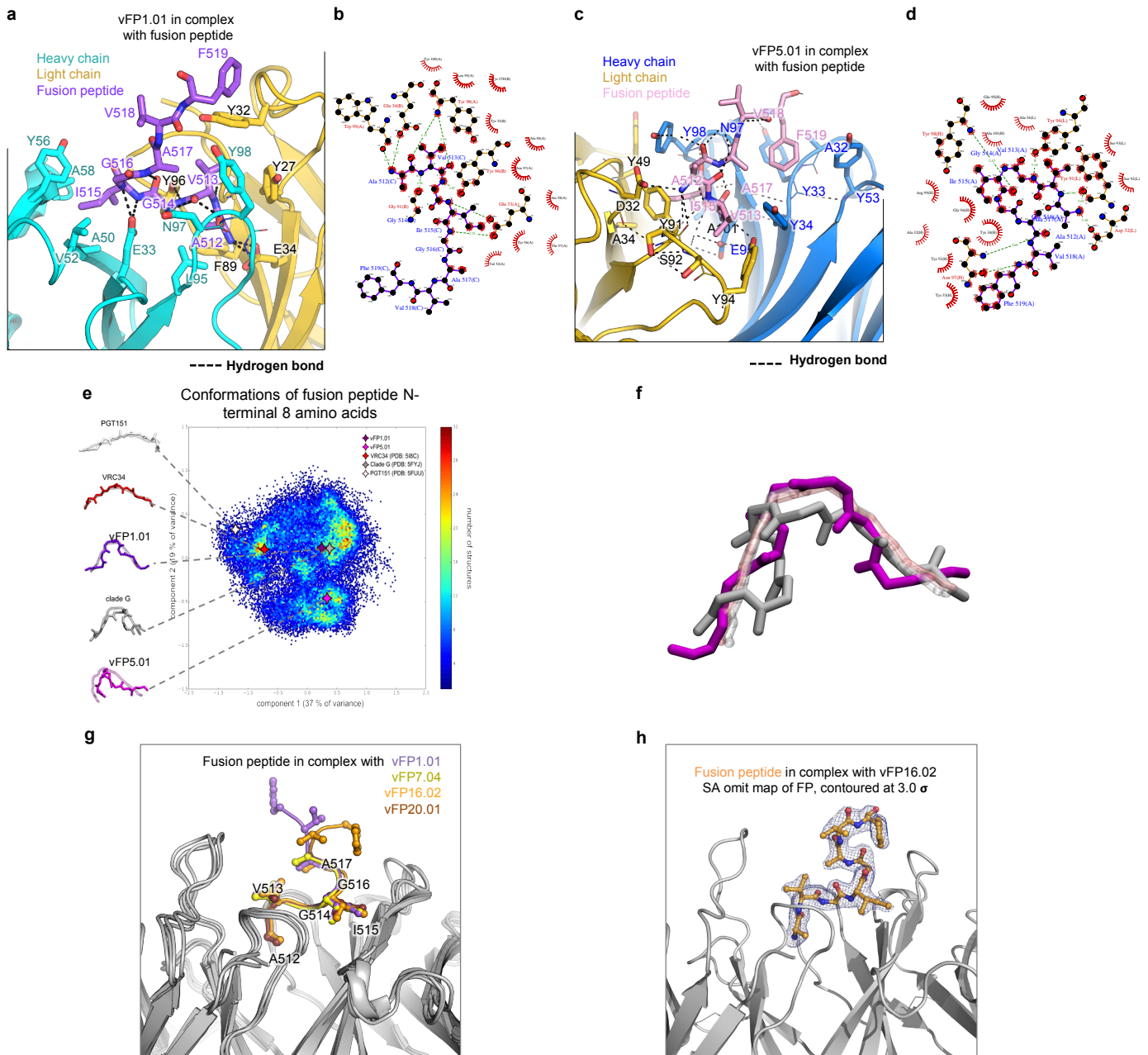
Mouse 1868

Class	Antibody	Heavy			Light				
		HV	HJ	HV identity (%)	CDR H3	KV	KJ	KV identity (%)	CDR L3
	vFP1.01	HV1-15*01	HJ1*03	94.5	LRNYWYFDV	KV1-117*01	KJ2*01	95.6	FQGSHVPYT
	vFP1.02	HV1-15*01	HJ1*03	94.5	LRNYWYFDV	KV1-117*01	KJ2*01	95.9	FQGSHVPYT
vFP1	vFP2.01	HV1-15*01	HJ2*01	96.5	LKRFYYFDY	KV1-117*01	KJ4*01	93.2	FQGSHVPYT
	vFP3.01	HV1-15*01	HJ2*01	95.2	LKRFYYFDY	KV1-117*01	KJ4*01	95.6	FQGSHFPFT
	vFP4.01	HV1-12*01	HJ1*03	94.6	LLPKWYFDV	KV1-117*01	KJ2*01	96.9	FQGSHVPYT
vFP5	vFP5.01	HV3-6*01	HJ3*01	94.9	EGNYRAY	KV6-23*01	KJ5*01	93.2	QQYSSYPLT
vFP6	vFP6.01	HV1-7*01	HJ2*01	93.1	GYVAFHY	KV2-112*01	KJ4*01	97.6	QLVQHPFT

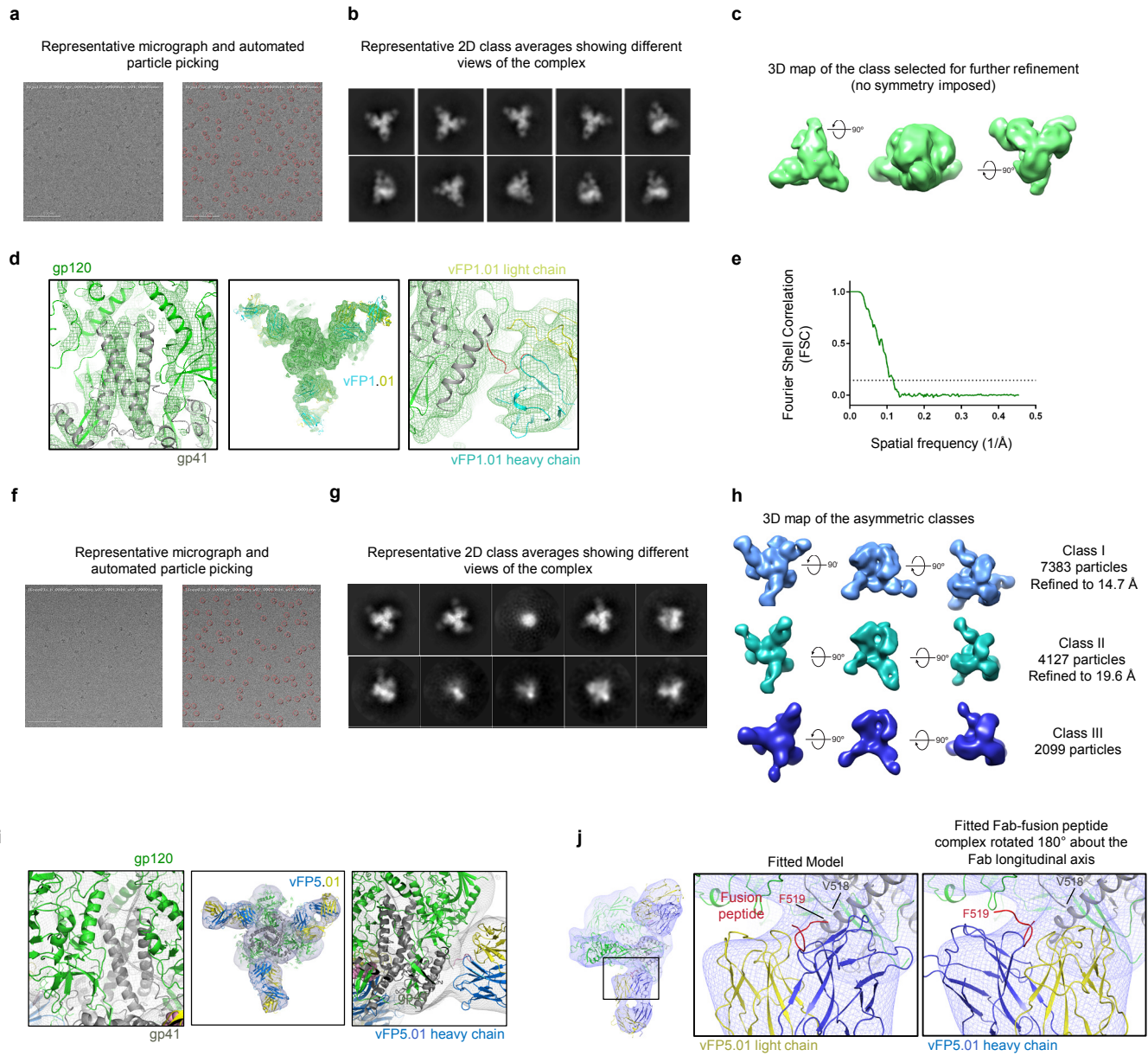
Mouse 2586									
		HV	HJ	HV identity (%)	CDR H3	KV	KJ	KV identity (%)	
	vFP7.01	HV1-15*01	HJ1*03	96.5	LRLYGYFDV	KV1-117*01	KJ2*01	99.0	FQGSHVPYT
	vFP7.02	HV1-15*01	HJ1*03	96.9	LRLYGYFDV	KV1-117*01	KJ2*01	98.6	FQGSHVPYT
vFP1	vFP7.03	HV1-15*01	HJ1*03	96.5	LRLYWYFDV	KV1-117*01	KJ2.01	99.3	FQGSHVPYT
	vFP7.04	HV1-15*01	HJ1*03	97.9	LRLYWYFDV	KV1-117*01	KJ2*01	98.0	FQGSHVPYT
	vFP7.05	HV1-15*01	HJ1*03	96.2	LRLYWYFDV	KV1-117*01	KJ2*01	96.6	FQGSHVPYT

b**c**

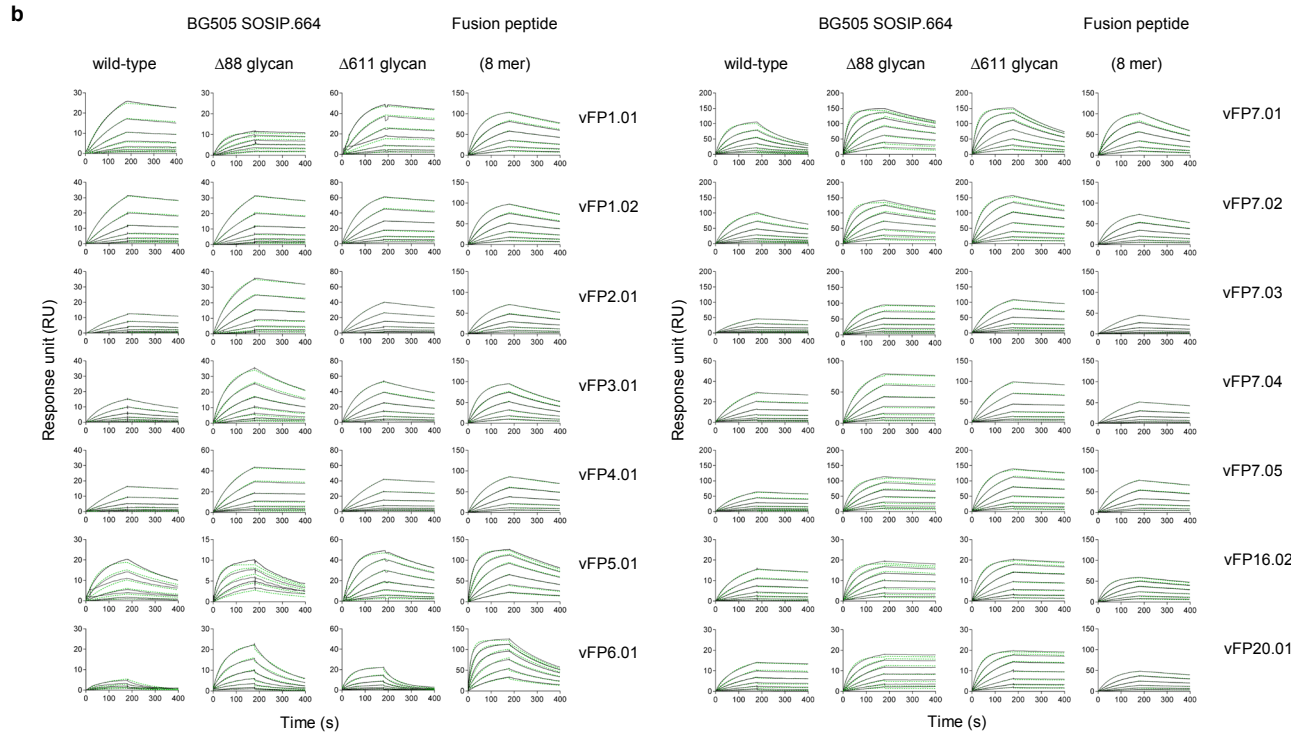
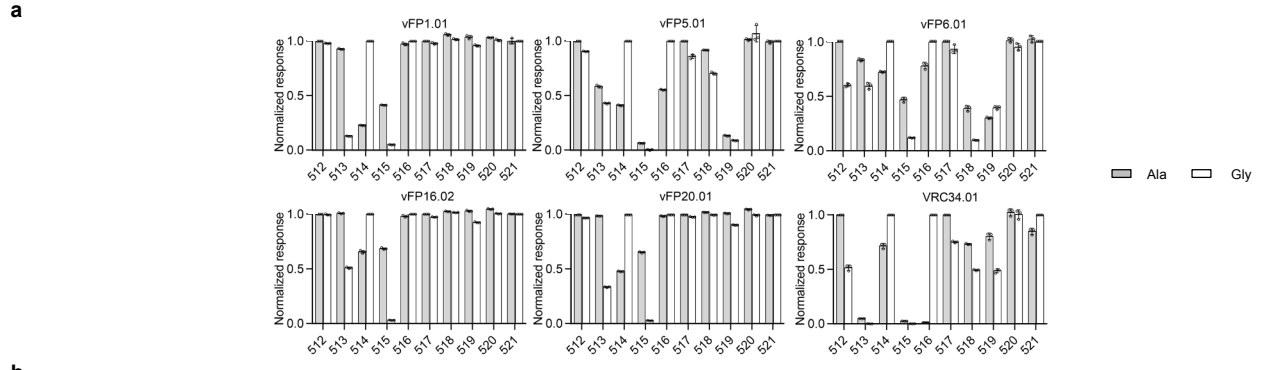
Supplementary Figure 3. First generation vaccine-elicited antibodies targeting FP neutralize up to ~10% of HIV-1 strains. **a**, Genetic characteristics of vaccine-elicited antibodies recognizing both HIV-1 Env and FP. Identity values are based on nucleotide sequence of the indicated heavy or light chain gene. **b**, Heavy and light chain phylogenetic tree. **c**, Neutralization dendograms tested on 208-isolate panel for vaccine-elicited antibodies vFP1.01, vFP5.01 and vFP7.04, with branches only shown for neutralized strains and colored according to neutralization potency. Strains sensitive to V3-directed or CD4-induced antibodies shown in italics. See Supplementary Table 3a for titers.



Supplementary Figure 4. Structural details of FP-conformational diversity and recognition by antibody. **(a-b)** vFP1.01 crystal structure with FP. **a**, Interaction between vFP1.01 and FP (contacting residues are shown as sticks). **b**, Ligplot showing the contact between vFP1.01 and FP. **(c-d)** vFP5.01 crystal structure with FP. **c**, Interaction between vFP5.01 and FP (contacting residues are shown as sticks). **d**, Ligplot showing the contact between vFP5.01 and FP. **e**, Principal component analysis of FP conformation based on molecular dynamics simulations of fully glycosylated HIV-1-Env trimer. Principal component projections (in transparency) are shown for HIV-1-fusion peptides bound by antibody (or for clade G Env trimer-5FYJ). Four prevalent clusters of fusion-peptide conformations were observed. Most prevalent was a symmetrical U-shaped conformation, which was recognized by FP1.01 and also observed in the fully glycosylated Env trimer from a Clade G isolate. A J-shaped conformation, recognized by FP5.01, was also highly prevalent, as was the extended linear conformation, recognized by VRC34.01. A related extended conformation was also recognized by antibody PGT151, though the conformational space sampled by the PGT151-bound antibody was substantially less dense than the other antibody-recognized conformations. **f**, Conformational superposition of the peptides analyzed in (e), along with the principal component projection (in transparency). Despite substantial difference in secondary structure, the two conformations share similar global shape. Thus, even though the FP-conformation in 5FYJ is slightly helical (one turn), both peptides adopt a symmetrical "U"-shape conformation. **g**, Superimposition of vFP1-class antibodies in complex with FP (residues 512-519). Antibody variable regions of vFP1-class antibodies, including vFP1.01, vFP7.04, vFP16.02 and vFP20.01, were aligned structurally. **h**, SA omit map of FP, in the crystal structure of vFP16.02 bound complex.



Supplementary Figure 5. Cryo-EM details for reconstructions of up to 8.6\AA resolution. (a-e) Details of cryo-EM structure of vFP1.01 complex with BG505 SOSIP trimer. **a**, Representative micrograph (left) with particles picked with DogPicker shown in red circles (right). **b**, Representative 2D class averages. **c**, Views of the 3D class selected for refinement. **d**, Snapshot of density and fit of model at different regions of the complex. The panel on the left is shown at a higher map contour than the other two panels to highlight the fit around the gp41 region of the trimer, which is one of the most well-defined regions of the complex. **e**, Fourier shell correlation plot for the 3D refinement ($\text{FSC}_{0.143} = 8.6\text{\AA}$, indicated by the dotted line). (f-i) Details of cryo-EM structure of vFP5.01 complex with BG505 SOSIP trimer. **f**, Representative micrograph (left) with particles picked with DogPicker shown in red circles. **g**, Representative 2D class averages. **h**, Views of asymmetric 3D classes. **i**, Snapshot of refined Class I density and fit of model at different regions of the complex. **j**, Comparison of the orientation of the vFP5.01 Fab-fusion peptide crystal structure fitted into the cryo-EM map, with its orientation rotated 180° about the longitudinal axis of the Fab. In the fitted model, residue Phe519 of the fusion peptide bound to the Fab in the crystal structure is favorably placed near residue Val518 of the fitted trimer, whereas in the 180° rotated model, Phe519 diverges away from the electron density and gp41 in the fitted trimer. Cryo-EM data collection was performed once for each structure. The represented images in (a, b, f and g) was derived from the analysis of many particles in many images. Additional details on cryo-EM data collection, such as total number of particles, number of images, can be found in Supplementary Table 4.



c

Ligand	BG505.DS.SOSIP			BG505.DS.SOSIP. Δ 88			BG505.DS.SOSIP. Δ 611			Fusion peptide		
	ka (1/Ms)	Kd (1/s)	KD (M)	ka (1/Ms)	Kd (1/s)	KD (M)	ka (1/Ms)	Kd (1/s)	KD (M)	ka (1/Ms)	Kd (1/s)	KD (M)
vFP1.01	4.73E+04	6.07E-04	1.28E-08	1.45E+05	3.04E-04	2.10E-09	9.02E+04	4.47E-04	4.96E-09	1.89E+05	1.35E-03	7.15E-09
vFP1.02	3.80E+04	4.77E-04	1.25E-08	1.01E+05	1.14E-04	1.13E-09	6.62E+04	3.89E-04	5.87E-09	1.66E+05	1.36E-03	8.19E-09
vFP2.01	2.43E+04	6.61E-04	2.72E-08	5.38E+04	4.24E-04	7.87E-09	3.69E+04	9.15E-04	2.48E-08	9.53E+04	1.48E-03	1.56E-08
vFP3.01	4.34E+04	2.20E-03	5.07E-08	7.64E+04	2.23E-03	2.95E-08	6.49E+04	1.47E-03	2.26E-08	1.91E+05	2.76E-03	1.44E-08
vFP4.01	1.93E+04	4.36E-04	2.26E-08	4.99E+04	1.92E-04	3.85E-09	2.92E+04	3.90E-04	1.33E-08	1.04E+05	1.02E-03	9.82E-09
vFP5.01	6.75E+04	3.10E-03	4.62E-08	2.23E+05	3.66E-03	1.64E-08	1.24E+05	1.88E-03	1.51E-08	3.88E+05	2.06E-03	5.29E-09
vFP6.01	1.12E+04	1.04E-02	9.28E-07	6.55E+04	5.72E-03	8.74E-08	1.55E+05	2.61E-02	1.69E-07	6.65E+05	3.48E-03	5.23E-09
vFP7.01	1.90E+05	5.14E-03	2.71E-08	3.00E+05	1.34E-03	4.46E-09	2.25E+05	3.12E-03	1.39E-08	4.79E+06	2.54E-03	5.30E-10
vFP7.02	7.22E+04	1.97E-03	2.72E-08	1.90E+05	1.19E-03	6.26E-09	1.34E+05	1.02E-03	7.61E-09	3.29E+06	1.48E-03	4.50E-10
vFP7.03	4.22E+04	6.10E-04	1.44E-08	8.83E+04	1.59E-04	1.80E-09	6.25E+04	5.59E-04	8.94E-09	1.26E+06	1.25E-03	9.94E-10
vFP7.04	5.07E+04	3.48E-04	6.86E-09	8.20E+04	1.32E-04	1.61E-09	5.55E+04	3.10E-04	5.59E-09	1.11E+06	8.94E-04	8.05E-10
vFP7.05	5.71E+04	4.38E-04	7.68E-09	1.59E+05	3.29E-04	2.07E-09	9.59E+04	4.11E-04	4.28E-09	2.52E+06	7.68E-04	3.05E-10
vFP16.02	5.82E+04	4.18E-04	7.19E-09	1.79E+05	3.11E-04	1.74E-09	1.41E+05	2.96E-04	2.10E-09	9.87E+05	1.05E-03	1.06E-09
vFP20.01	5.99E+04	2.22E-04	3.71E-09	1.49E+05	6.33E-05	4.26E-10	1.57E+05	1.47E-04	9.34E-10	5.88E+05	9.61E-04	1.64E-09
VRC34	5.25E+05	3.40E-04	6.48E-10	1.63E+06	3.27E-03	2.00E-09	1.59E+06	7.09E-04	4.46E-10	1.50E+06	9.24E-03	6.17E-09

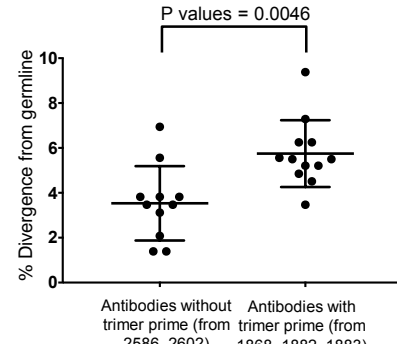
Supplementary Figure 6. Binding of vaccine-elicited antibodies to HIV-1 Env trimers and His-tagged FP. **a**, Bar plots of Ala/Gly scan. Binding of indicated antibodies to alanine (grey bars) and glycine (white bars) mutants are shown, normalized by binding to the wild-type sequence. FP amino acids are shown on x-axis. Experiments were performed in triplicate ($n=3$ independent experiments), error bars indicating mean with SD are plotted for each residue position in the overlaid scatter dot plot. See Supplementary Table 5 for numerical details and additional vFP1-class antibodies. **b**, SPR sensorgrams of vFP1.01, vFP1.02, vFP2.01, vFP3.01, vFP4.01, VFP5.01, VFP6.01, vFP7.01, vFP7.02, vFP7.03, vFP7.04, vFP7.05, vFP16.02 and vFP20.01 binding to wild type, glycan-deleted BG505.DS-SOSIP trimers and His-tagged FP. Blank-corrected sensograms were shown in black and fitted data using a 1:1 Langmuir model of binding were shown in green dashed lines. **c**, SPR constants of all first and second generation vFPs Fabs binding to wild type, glycan-deleted BG505.DS-SOSIP, and FPs.

a

Mouse ID	Immunization			SVA-MLV		BG505 WT		BG505 Δ611 glycan		BG505 Δ88+Δ611 glycans		Hybridoma-identified antibodies					
	1	2	3	ID ₅₀	ID ₈₀	ID ₅₀	ID ₈₀	ID ₅₀	ID ₈₀	ID ₅₀	ID ₈₀	(All vFP1 class)					
2586	FP8	FP8		23	<20	<20	<20	78	<20	239	<20	vFP7.01-vFP7.03, vFP7.04-vFP7.07, vFP7.08					
2602	FP8	FP8		<20	<20	60	<20	275	22	575	55	vFP8.01, vFP8.02, vFP8.03					
1868	T1	FP8	FP8	50	<20	<20	<20	108	20	493	65	vFP1.01-vFP1.02, vFP2.01, vFP3.01, vFP4.01					
1882	T1	FP8	FP8	23	<20	<20	<20	95	<20	320	26	vFP9.01					
1883	T1	FP8	FP8	25	<20	<20	<20	62	<20	239	29	vFP10.01-vFP10.05, vFP11.01					

Key:
FP8 = AVGIGAVF-KLH
T1 = BG505 SOSIP

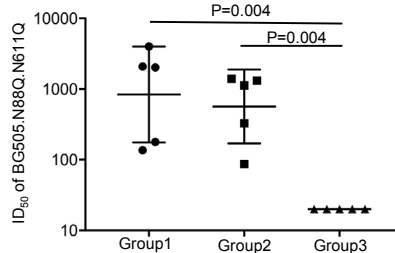
ID ₅₀	ID ₈₀
<40	<20
40-100	20-100
100-1000	

b**c**

Group #	Immunizations						BG505.N88Q.N611Q													
	1	2	3	4	5	6	Animal ID	ID ₅₀	ID ₈₀											
1	T1	FP8	FP7	FP6	T2	T2	4441	2029	280											
							4442	136	<20											
							4443	2087	348											
							4444	4011	488											
							4445	178	<20											
							4446	1398	222											
2	T1	FP8	FP8	FP8	T2	T2	4447	87	<20											
							4448	1127	325											
							4449	329	62											
							4450	1312	302											
							4451	<20	<20											
3	T1	KLH only	KLH only	KLH only	T2	T2	4452	<20	<20											
							4453	<20	<20											
							4454	<20	<20											
							4455	<20	<20											

Key:
FP8 = AVGIGAVF-KLH
FP6 = AVGIGA-KLH
T1 = BG505 SOSIP
T2 = BG505 DS SOSIP

ID ₅₀	ID ₈₀
<40	<20
40-100	20-100
100-1000	
1000-10000	
>10000	

d**e**

Week 18 sera neutralization of the guinea pig group, immunized with only 3x BG505.DS.SOSIP Env trimer

Clade	A		A		B		B		C		AE		BC		C		C		A		A		A		Wild type viruses neutralization #/10 in ID ₅₀
	Glycan missing	Complete	241+611	448	241	241	241	241	241	241	88+241	241+611	88+241+611	BG505 Δ88	BG505 Δ611										
Guinea pig ID	ID ₅₀	ID ₈₀	ID ₅₀	ID ₅₀	ID ₈₀																				
CGP606-1	<20	<20	<20	<20	<20	<20	<20	<20	<20	<20	<20	<20	<20	<20	<20	<20	<20	6,910	765	7,461	745	8,931	2,474	8,494	1,249
CGP606-2	<20	<20	<20	<20	<20	<20	<20	<20	<20	<20	<20	<20	<20	<20	<20	<20	<20	2,434	330	1,149	205	5,499	1,608	2,736	502
CGP606-3	<20	<20	<20	<20	<20	<20	<20	<20	<20	<20	<20	<20	<20	<20	<20	<20	<20	20,000	3,972	20,000	4,045	20,000	4,914	20,000	5,018
CGP606-4	<20	<20	-*	-*	-*	-*	-*	-*	-*	-*	-*	-*	-*	-*	-*	-*	-*	1,324	260	684	88	5,998	887	3,874	172
CGP606-5	<20	<20	<20	<20	<20	<20	<20	<20	<20	<20	<20	<20	<20	<20	<20	<20	<20	1,315	288	611	119	5,394	2,026	2,583	309

* No enough sera to test

<20

20-100

100-1000

1000-10000

>10000

f

Week 18 sera neutralization of the NHP group, immunized with only 3x BG505.DS.SOSIP Env trimer

Clade	A		A		B		B		C		AE		BC		C		C		A		A		A		Wild type viruses neutralization #/10 in ID ₅₀	
	Glycan missing	Complete	241+611	448	241	241	241	241	241	241	88+241	241+611	88+241+611	BG505 D88	BG505 D611											
NHP ID	ID ₅₀	ID ₈₀	ID ₅₀																							
A12V163	<20	<20	<20	<20	<20	<20	<20	<20	<20	<20	<20	<20	<20	<20	<20	<20	<20	<20	<20	<20	<20	<20	<20	123	0	
A12V193	<20	<20	<20	<20	<20	<20	<20	<20	<20	<20	<20	<20	<20	<20	<20	<20	<20	42	104	139	27	363	74	0	1	
A12V168	<20	<20	<20	<20	<20	<20	<20	<20	<20	<20	290	118	45	27	<20	<20	<20	307	104	572	155	742	226	0	3	
A12V049	<20	<20	<20	<20	<20	<20	<20	<20	<20	<20	<20	<20	<20	<20	<20	<20	<20	1,034	272	787	251	909	278	1,280	447	1
A12V145	<20	<20	<20	<20	<20	<20	<20	<20	<20	<20	<20	<20	<20	<20	<20	<20	<20	<20	<20	<20	<20	<20	<20	70	0	

<20

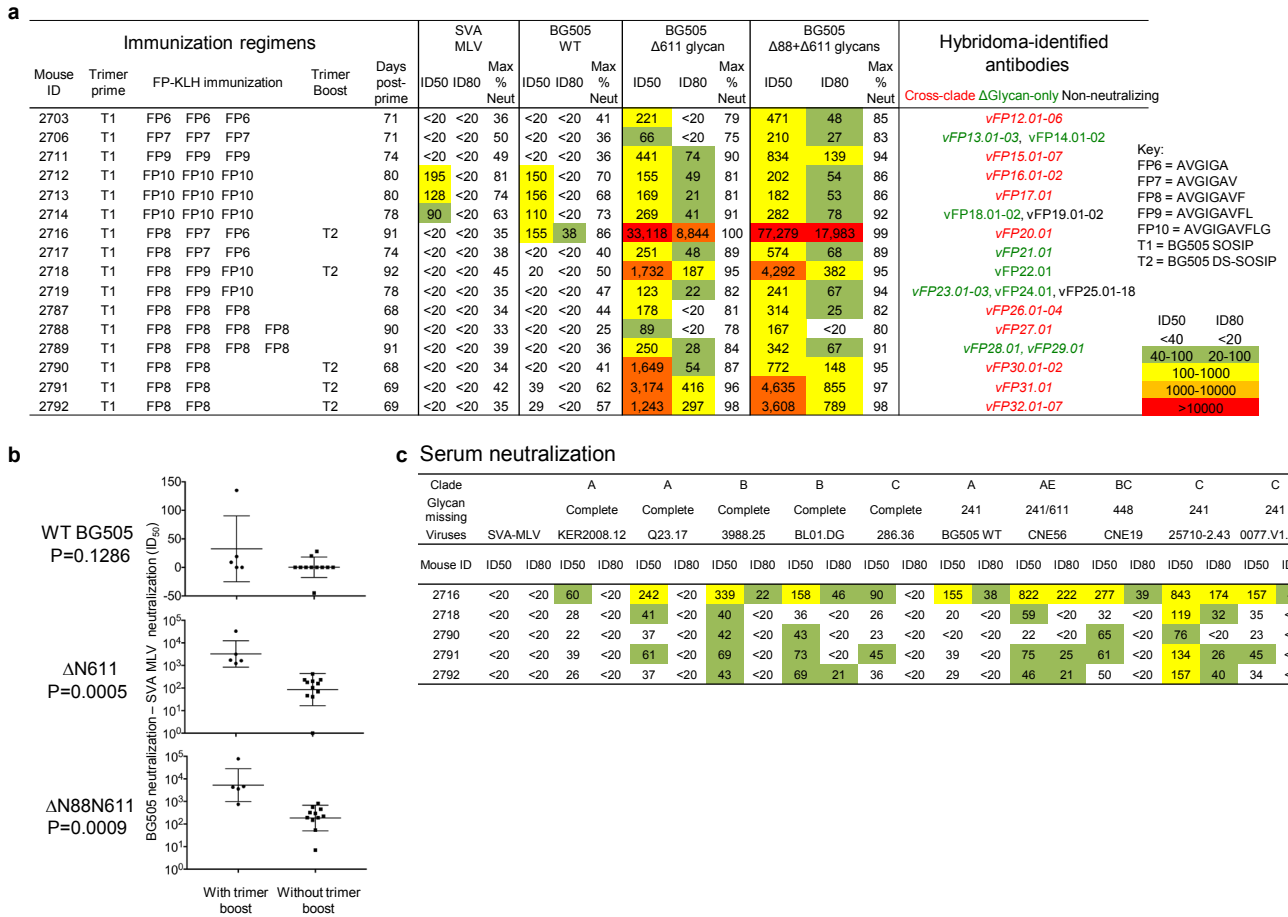
20-100

100-1000

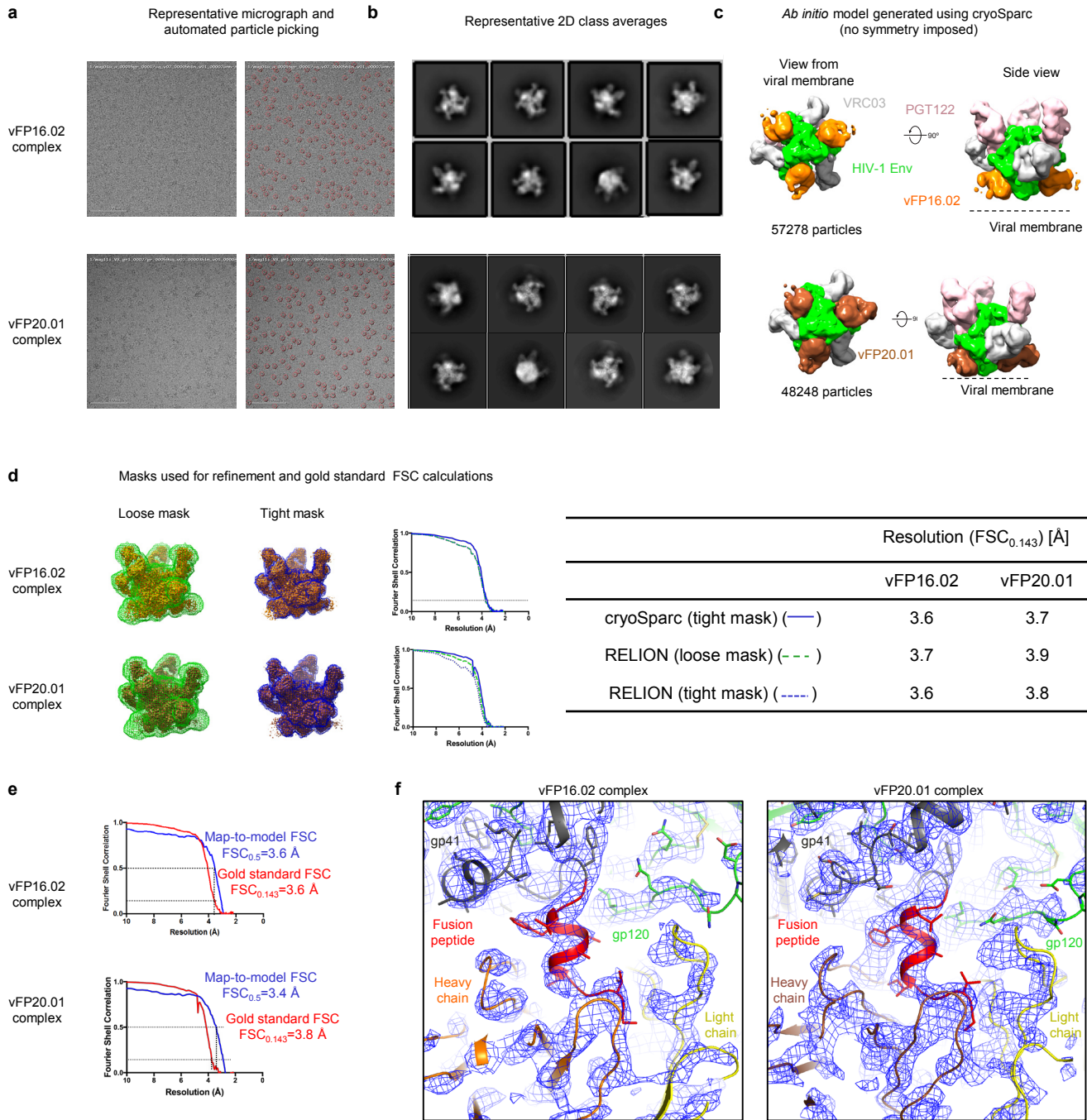
1000-10000

>10000

Supplementary Figure 7. Comparator mouse, guinea pig and NHP immunization experiments. **a**, FP8-KLH mouse immunizations with or without Env-tr



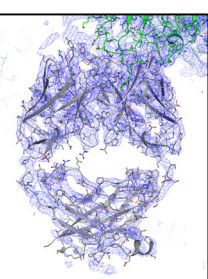
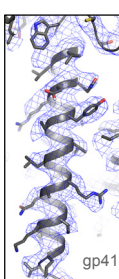
Supplementary Figure 8. Second-generation murine immunization schema and elicited serum neutralization. **a**, 16 mice and 11 immunization schema (left), with neutralization (middle) and hybridoma-identified antibodies (right). Names for vFP1-class antibodies are italicized and colored according to neutralization properties as indicated. **b**, Trimer boost induced significantly higher serum neutralization titers by two-tailed Mann-Whitney. n=5 for “with trimer boost” group and n=11 for “without trimer group boost”; mean and SD were displayed for WT BG505 panel, and geometric mean and geometric SD were displayed for the other two panels. **c**, Neutralization by trimer-boosted sera on 10 wildtype isolates, 5 with complete glycans around FP and 5 naturally missing select glycans as specified, with ID50/ID80 colored as in (a). **d**, Neutralization dendograms. Top row: 208-isolate panel for vaccine-elicited antibodies vFP16.02 and vFP20.01,



Supplementary Figure 9. Cryo-EM structural details for reconstructions of better than 4 Å resolution. **(a-f)** Details of cryo-EM structures of vFP16.02-BG505 DS-SOSIP-VRC03-PGT122 and vFP20.01-BG505 DS-SOSIP-VRC03-PGT122 complexes. **a,** Representative micrograph (left) with particles picked with DogPicker shown in red circles (right). **b,** Representative 2D class averages. **c,** *Ab initio* models generated using cryoSpaC. **d,** Refined map in orange with the mask used for the final iteration of cryoSpaC refinement (green) and for FSC calculation (blue) shown as mesh. FSC plots and resolution values reported by cryoSpaC and RELION according to the gold standard FSC_{0.143} criterion (FSC_{0.143} shown as dotted line). **e,** Gold standard (red) and map-to-model (blue) FSC correlation curves. The map-to-model FSC curve was calculated for protein residues within the complex excluding the antibody constant domains. **f,** Zoomed-in view of the region around the fusion peptide with electron density shown in blue mesh. Cryo-EM data collection was performed once for each structure. The represented images in **(a and b)** was derived from the analysis of many particles in many images. Additional details on cryo-EM data collection, such as total number of particles, number of images, can be found in Supplementary Table 4.

a Representative electron density in vFP16.02.DS.SOSIP-VRC03-PGT122 reconstruction

Density contoured to show
gp41 helical pitch and side
chains*



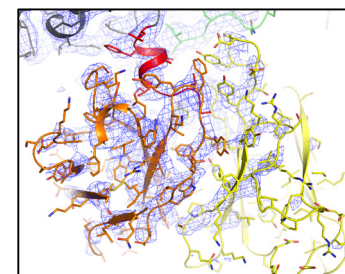
VRC03*

PGT122*

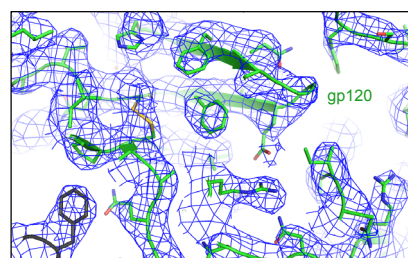
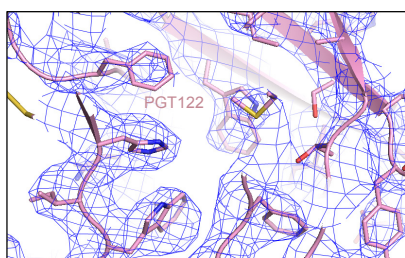
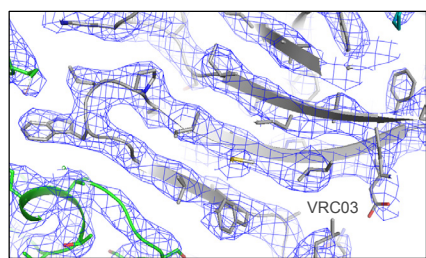
vFP16.02*

Heavy chain
Light chain

Zoom-in the fusion peptide *showing
ordered vFP16.02 electron density around

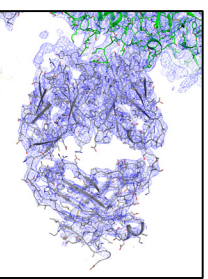
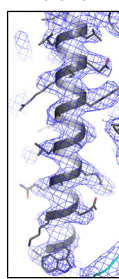


*Electron density (blue mesh) in all five images above are contoured at the same level.



b

Density contoured to show
gp41 helical pitch and side
chains#

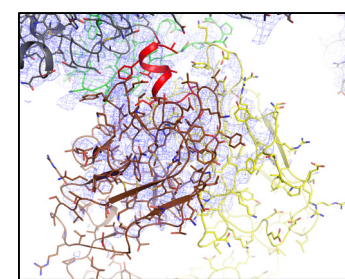


VRC03 #

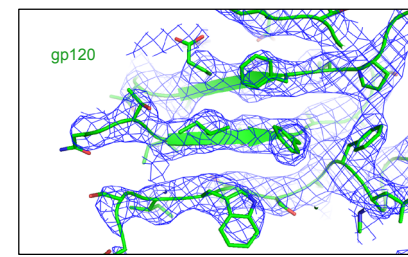
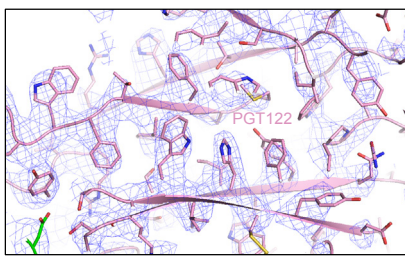
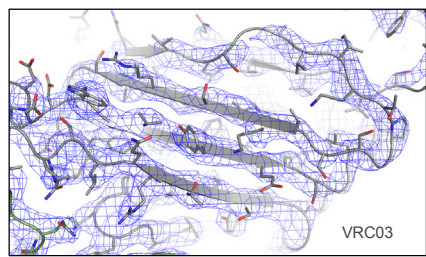
PGT122 #

vFP20.01 #

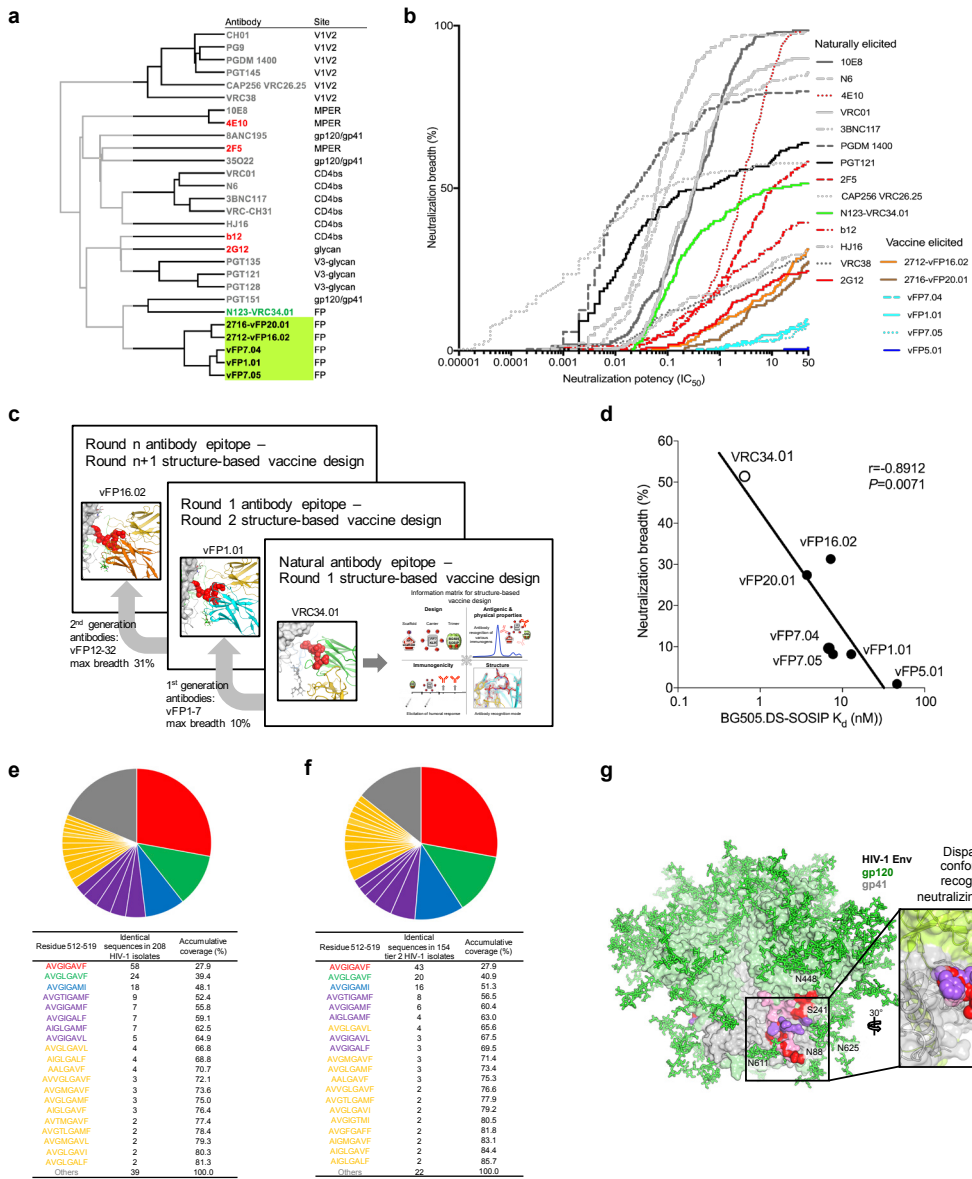
Zoom-in showing ordered vFP20.01
electron density around the fusion peptide #



Electron density (blue mesh) in all five images above are contoured at the same level.

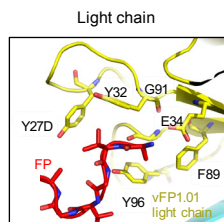
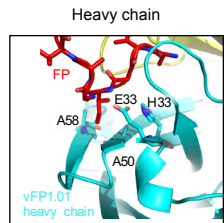


Supplementary Figure 10. Cryo-EM reconstructions reveal focused recognition of the HIV-1 fusion peptide by antibodies vFP16.02 and vFP20.01. a, Top panel. Focused recognition of fusion peptide by vFP16.01. Bottom panel. Representative electron density plots from different regions of the vFP16.02-DS.SOSIP-VRC03-PGT122 structure. **b,** Same as **a**, but for the vFP20.01-DS-SOSIP-VRC03-PGT122 complex.

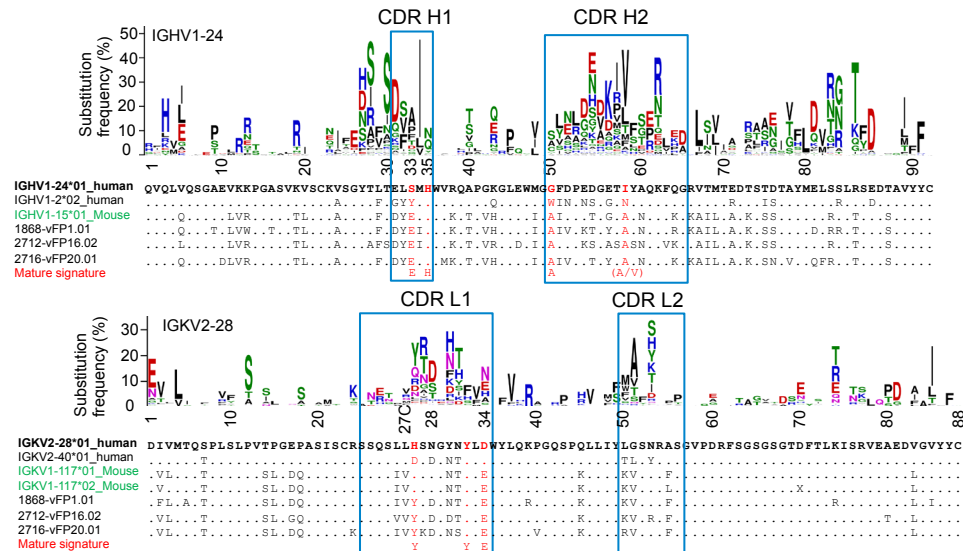


Supplementary Figure 11. Iterative epitope-based vaccine development to achieve neutralization of heterologous viral strains. **a**, Dendrogram representing neutralization fingerprints shows vaccine-elicited antibodies to cluster with FP antibodies isolated from HIV-1 infected donors, though as a separate group. **b**, Comparison of HIV-1-neutralization breadth and potency by antibodies isolated from HIV-1 infected donors to vaccine-elicited antibodies. **c**, Schematic showing process of iterative structure-based vaccine design, which involves analysis of elicited antibodies to provide insight into the design and improvement of immunogens and immunization regimens for subsequent cycles of improvement. **d**, Neutralization breadth of FP-directed antibodies versus affinity for stabilized Env trimer. Pearson correlation was displayed, $n=7$ antibodies. **e**, Sequence diversity of the N-terminal eight residues of FP (residue 512 to 519) in the 208-isolate panel, in pie chart format (top) and table format ranked by their prevalence (bottom). The accumulative coverage of the sequence diversity of these five residues is also shown. **f**, Same as (e), but with 154 isolates resistant to neutralization by CD4-induced antibodies, V3-directed antibodies, and F105 antibody. **g**, vFP-defined site of vulnerability allows for target-site conformational diversity.

a V-gene signature of vFP1 class antibodies

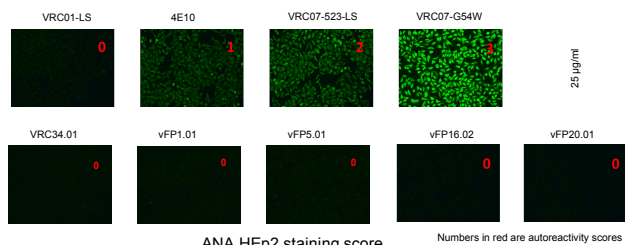


b Comparisons of IGHV1-15 and IGKV1-117 to their respective human homologs



c

ANA HEp2 staining assay



d

Anti-cardiolipin ELISA

mAb	OD			Interpretation
	100 µg/ml	33 µg/ml	100 µg/ml	
vFP1.01	0.21	0.1	20.62	8.18 Not reactive
vFP5.01	0.06	0.05	3.4	2.8 Not reactive
vFP16.02	0.04	0.04	-4.08	-4.56 Not reactive
vFP20.01	0.23	0.09	8.86	-0.62 Not reactive
VRC34.01	0.04	0.04	2.03	1.96 Not reactive
VRC01-LS	0.09	0.06	7.05	3.98 Not reactive
4E10	1.48	1.48	164.32	164.26 Reactive
VRC07-523-LS	0.11	0.06	9.49	4.2 Not reactive
VRC07-G54W	0.31	0.13	31.87	11.96 Not reactive

GPL color score

<15	Negative
15-20	indeterminate
20-80	low to medium positive
>80	high positive

Supplementary Figure 12. vFP1-class antibodies: V-gene similarity to human homologues and autoreactivity. **a**, V-gene signature of vFP1 class antibodies. Signature residues for heavy chain (top) and light chain (bottom) are shown in sticks and labeled. **b**, Comparisons of IGHV1-15 and IGKV1-117 to their respective human homologs identified by IMGT/V-QUEST and mutation profile of human gene IGHV1-24 and IGKV2-28. Compared to mouse IGHV1-15, human IGHV1-24 contains the H35 signature, and the A50 and A/V58 signatures can be reproduced by somatic hypermutation with high frequencies (See gene-specific substitution profile of IGHV1-24 built from 190 mature human antibody lineages, with one sequence per lineage). This suggested similar key signatures may be reproduced by human antibodies. However, the alignment also showed multiple germline gene positions are diversified between the homolog genes, further investigations are required to understand whether they will affect FP recognition. The mouse IGKV1-117 was aligned to two human kappa chain genes, IGKV2-28 and IGKV2-40. Similar to mouse IGKV1-117, the IGKV2-28 also has a His-Ser-Asn motif in CDR L1. We built a substitution profile for IGKV2-28 using 104 antibody lineages derived from repertoires of three healthy human donors. The substitution profile showed that the key signatures of vFP1 antibodies, Y27d, Y32, and E34 are either germline residue or mutations with high frequency in human IGKV2-28 antibodies, suggesting the signatures observed in the vFP1 antibodies can be obtained with high frequency. V gene positions numbered using Kabat system. **(c-d)** Autoreactivity analysis of FP-directed antibodies. **c**, ANA Hep-2 staining analysis showed none of the five FP-directed antibodies are autoreactive. Control antibodies with known autoreactivity are italicized. The experiment was performed twice (n=2) independently. **d**, Anti-cardiolipin ELISA showed none of the three FP-directed antibodies to be reactive. Control values italicized as in (c). The experiment was performed only once.

Supplementary Table 1. Amino acid sequences and alignment of vFP antibodies.

a. Amino acid sequence alignment of heavy chain variable region.

b. Amino acid sequence alignment of light chain variable region.

CDR regions are defined according to Kabat numbering system. We define antibody lineages to be members of the same antibody class if lineage members have the same mode of recognition and utilize similar B cell pathways of development (Kwong and Mascola, 2012).

Supplementary Table 2. V(D)J recombination of vFP lineages. (continued on next page)

a

Germline nucleotide and amino acid residues are shown in black with the corresponding junctions colored in light blue. Somatic hypermutation events are colored red. Nucleotides deleted by exonuclease trimming are crossed out. The N, P additions occurring at the junctions and the gene assignment are from IMGT Vquest (http://www.imgt.org/IMGT_Vquest/share/textes/).

Supplementary Table 2. V(D)J Recombination of vFP lineages. (continued from prior page)

b

1868		Light chain						2706		Light chain					
		vFP1.01	0	15	15	0	132	93		vFP13.01	0	0	65	65	
		vFP1.02	0	15	15	0	132	93		vFP13.02	13	0	65	65	
		vFP2.01	20	20	0	15	143	96		vFP13.03	13	0	65	65	
		vFP3.01	17	17	3	15	143	96		vFP14.01	66	62	62	0	
		vFP4.01	41	41	56	58	132	93		vFP14.02	65	60	60	2	
		vFP5.01	177	177	174	174	179								
		vFP6.01	81	81	63	66	76	173							
		Heavy chain								Heavy chain					
1883		Light chain						2714		Light chain					
		vFP10.01	0	0	0	0	0			vFP18.01	0	73	73		
		vFP10.02	1	0	0	0	0			vFP18.02	0	73	73		
		vFP10.03	3	2	0	0	0			vFP19.01	148	148	0		
		vFP10.04	3	2	0	0	0			vFP19.02	148	148	0		
		vFP10.05	1	0	2	2	0								
		vFP11.01	31	31	31	31	31								
		Heavy chain								Heavy chain					
2719		Light chain						2789		Light chain					
		vFP23.01	0	0	65	0	8			vFP28.01	0				
		vFP23.02	0	0	65	0	8			vFP29.01	17				
		vFP23.03	0	0	65	0	8								
		vFP24.01	80	80	80	66	73	73							
		vFP25.01	85	85	85	62	8	8							
		vFP25.02	85	85	85	62	0	0							
		vFP25.03	85	85	85	62	0	0							
		vFP25.04	85	85	85	62	0	0							
		vFP25.05	85	85	85	62	0	0							
		vFP25.06	85	85	85	62	0	0							
		vFP25.07	85	85	85	62	0	0							
		vFP25.08	85	85	85	62	0	0							
		vFP25.09	85	85	85	62	0	0							
		vFP25.10	85	85	85	62	0	0							
		vFP25.11	85	85	85	62	0	0							
		vFP25.12	85	85	85	62	0	0							
		vFP25.13	85	85	85	62	0	0							
		vFP25.14	83	83	83	60	21	21	21						
		vFP25.15	86	86	86	63	1	1	1						
		vFP25.16	81	81	81	66	10	10	10						
		vFP25.17	85	85	85	62	0	0	0						
		vFP25.18	85	85	85	62	0	0	0						
		Heavy chain								Heavy chain					

For each mouse with more than one vFP lineage, we performed pairwise comparison of nucleotide differences separating germline versions of heavy (blue) and light (yellow) chain variable regions. Mouse ID is listed in upper left of each table.

Supplementary Table 3. vFP antibody and sera neutralization.

a. vFP antibody neutralization against a panel of 208 isolates

	Annualized Standard Deviation	SD	CV	Alpha	Beta	Rho	Sharpe Ratio
Geometric Mean	9.61	44.9	11.7	51.9	8.00	5.82	
Mean	10.0	45.0	11.8	52.0	8.00	5.82	
SD	10.0	45.0	11.8	52.0	8.00	5.82	
CV	10.0	45.0	11.8	52.0	8.00	5.82	
Alpha	10.0	45.0	11.8	52.0	8.00	5.82	
Beta	10.0	45.0	11.8	52.0	8.00	5.82	
Rho	10.0	45.0	11.8	52.0	8.00	5.82	
Sharpe Ratio	10.0	45.0	11.8	52.0	8.00	5.82	

Note: Median and Geometric Mean titers are calculated only for viruses neutralized
Values "less than" the lowest concentration assayed were assigned that value for calculation purposes.

*To assess for non-specific neutralization at 500 ug/ml, the non-HIV-1 murine antibody 5C4 (specific for RSV neutralization) was tested at 500 ug/ml; two strains, HXB2.DG and DU123.06 were neutralized at 264 and 483 ug/ml, respectively, over 1000-fold less

Supplementary Table 3. vFP antibody and sera neutralization.

b. vFP antibody neutralization against a panel of 10 isolates.

HIV strains	IC50										IC80											
	KER2008.12	Q23.17	3988.25	BL01.DG	286.36	BG505.W6M		CNE56	CNE19	25710-2.43	0077.V1.C16	KER2008.12	Q23.17	3988.25	BL01.DG	286.36	BG505.W6M		CNE56	CNE19	25710-2.43	0077.V1.C16
						.C2	.C2									.C2	.C2					
1868-vFP1.01	19.1	3.01	>100	>50	>50	21.9	4.49	2.96	0.756	7.1		>50	>50	>100	>50	39.9	31.7	4.32	44.3			
2586-vFP7.07	28.3	24.6	>50	>50	>50	43.6	9.2	9.18	4.63	>50		>50	>50	40.4	>50	30.3	>50					
2602-vFP8.02	7.35	1.01	1.96	5.86	10.9	2.2	0.715	0.48	0.513	3.39		>50	>50	43.2	>50	22.9	2.92	3.36	2.26	12.1		
2602-vFP8.03	>50	21.3	17.9	>50	18.1	>50	12.5	36.8	18.4	>50		>50	>50	>50	>50	>50	>50	>50	>50			
2682-vFP9.01	6.29	6.83	>50	>50	>50	26.9	16	1.32	1.69	18.3		>50	>50	>50	>50	>50	8.97	8.49	>50			
2703-vFP12.01	>50	13.9	5.01	>50	>50	>50	25.9	>50	>50	>50		>50	>50	>50	>50	>50	>50	>50	>50			
2703-vFP12.02	>50	11.3	36.1	>50	>50	>50	8.04	7.53	8.13	38.5		>50	>50	>50	>50	>50	30.3	49.3	40.7	>50		
2703-vFP12.04	11.4	4.31	3.58	8.16	35.6	6.96	0.831	3.9	0.796	8.47		>50	>50	41.3	>50	>50	3.47	23.8	4.06	36.1		
2703-vFP12.06	36.1	28.2	5.67	32.6	>50	15.3	8.6	5.96	6.45	>50		>50	>50	49.1	>50	30.5	39.2	23.1	>50			
2711-vFP15.01	45.5	24.5	>50	>50	40.3	44.9	6.07	9.01	2.97	>50		>50	>50	>50	>50	31.1	>50	24.8	>50			
2711-vFP15.02	4.15	1.55	6.68	32.3	20	9.24	2.85	2.38	1.51	13.2		>50	>50	>50	>50	10.4	24.3	5.05	>50			
2711-vFP15.03	3.97	14.4	>50	>50	10.9	21.2	27.6	0.922	0.562	23.8		>50	>50	>50	>50	>50	7.42	2.05	>50			
2711-vFP15.04	19.8	5.16	>50	>50	>50	36.1	3.79	4.66	1.73	23.3		>50	>50	>50	>50	16.3	>50	9.56	>50			
2711-vFP15.05	23	6.39	4.75	>50	13.7	17.0	7.38	3.34	2.09	23.5		>50	>50	>50	>50	15.8	42.4	8.88	>50			
2711-vFP15.07	2.01	5.91	45.2	>50	18.2	>50	6.52	3.82	0.751	6.84		>50	>50	>50	>50	25.4	>50	3.03	44.3			
2712-vFP16.02	1.44	0.84	6.72	3.26	2.67	2.64	1.06	0.203	0.355	1.29		14	13.4	>50	14.3	35	9.31	3.6	0.888	1.21	3.83	
2713-vFP17.01	>50	350	7.2	12.3	>50	18.9	19.3	4.05	1.46	23.7		>50	>50	>50	>50	>50	>50	13	>50			
2716-vFP20.01	2.84	1.67	1.16	3.91	6.56	2.47	1.82	0.644	0.608	4.39		>50	40.7	>50	23.2	>50	8.15	6.96	3.63	3.39	20.3	
2787-vFP26.02	>50	15.1	8.51	>50	>50	28.5	17.1	23.1	3.95	18.5		>50	>50	>50	>50	>50	>50	>50	>50	>50		
2787-vFP26.03	3.96	27.7	>50	22.7	>50	39.2	8.43	0.539	0.574	9.46		>50	>50	>50	>50	29.6	3.54	2.37	>50			
2787-vFP26.04	4.25	2.91	8.42	19.8	28.8	6.04	10.8	1.3	1.23	15.2		>50	>50	>50	>50	25.7	>50	8.24	4.49	>50		
2788-vFP27.01	1.84	6.9	9.55	>50	24.8	16.4	11	1.45	1.03	28.2		>50	>50	>50	>50	46.3	11.1	5.41	>50			
2790-vFP30.01	5.48	3.18	9.71	7.39	40.2	1.73	4.17	2.12	2.03	7.28		>50	>50	42.3	>50	5.6	12.1	14.1	8.11	30.3		
2791-vFP31.01	7.05	1.92	14.8	17.3	36.9	21.5	3.92	1.27	1.14	9.7		>50	>50	>50	>50	21.6	7.47	3.5	>50			
2792-vFP32.01	35.9	30.4	>50	35.3	>50	9.38	10.7	2.86	3.13	11.2		>50	>50	>50	>50	32	40.6	17.4	12.7	40.8		
2792-vFP32.03	>50	33.1	>50	2.33	>50	0.751	1.11	7.93	1.27	2.53		>50	>50	17.9	>50	2.03	2.62	>50	8.05	11.8		
2792-vFP32.04	34.3	4.75	>50	8.55	>50	17.2	4.46	2.38	1.03	26.7		>50	>50	47.9	>50	>50	23	22.3	3.73	>50		
2792-vFP32.06	20.2	44.6	>50	>50	24.6	10.9	2.4	2.42	44.2		>50	>50	>50	>50	49.8	24.9	19.2	>50				
2792-vFP32.07	>50	8.49	>50	2.86	>50	1.67	1.17	10.7	1.14	2.93		>50	>50	23.9	>50	6.09	3.66	>50	7	15.4		
N123-VRC34.01	0.028	0.083	0.028	0.048	4.11	0.069	>50	0.033	0.128	0.721		0.138	0.36	0.111	0.193	>50	0.331	>50	1.54	6.22	24.2	

Supplementary Table 3. vFP antibody and sera neutralization.

c. NHP sera neutralization against a panel of 58 isolates with matching FP sequence in the first 8 residues to the immunogens and naturally missing glycans highlighted in gray.

Supplementary Table 4. Data collection and refinement statistics.

a. Crystal data collection and refinement statistics (molecular replacement)

PDB accession code	vFP1.01:FP 5TKJ	vFP5.01:FP 5TKK	vFP7.04:FP 6CDM	vFP16.02:FP 6CDO	vFP20.01:FP 6CDP
Data collection					
Space group	P 2 ₁ 2 ₁ 2 ₁	P 2 ₁	P 2 ₁	P 4 ₁ 2 ₁ 2	C 2 2 2 ₁
Cell dimensions					
<i>a, b, c</i> (Å)	76.16, 120.18, 226.18	36.24, 82.23, 72.26	79.57, 61.03, 88.65	141.03, 141.03, 77.64	60.46, 192.31, 87.56
α, β, γ (°)	90.00, 90.00, 90.00	90.00, 90.23, 90.00	90.00, 91.89, 90.00	90.00, 90.00, 90.00	90.00, 90.00, 90.00
Resolution (Å)	50 - 2.12 (2.16 - 2.12)*	50 - 1.55 (1.58 - 1.55)	50 - 2.41 (2.49 - 2.41)	50 - 2.10 (2.17 - 2.10)	50 - 2.46 (2.54 - 2.46)
R_{sym} or R_{merge}	0.093 (0.517)	0.066 (0.468)	0.127 (0.412)	0.108 (0.931)	0.118 (0.423)
$I / \sigma I$	20.7 (2.4)	16.1 (2.1)	10.0 (2.0)	30.9 (2.2)	19.8 (2.1)
Completeness (%)	99.6 (97.8)	97.2 (85.2)	99.3 (94.1)	99.8 (98.3)	97.4 (83.2)
Redundancy	7.1 (5.4)	3.5 (2.1)	3.5 (2.8)	13.9 (9.7)	6.4 (4.9)
Refinement					
Resolution (Å)	43.54 - 2.12 (2.16 - 2.12)	25.47 - 1.55 (1.58 - 1.55)	44.3 - 2.41 (2.49 - 2.41)	41.95 - 2.10 (2.17 - 2.10)	48.17 - 2.46 (2.54 - 2.46)
No. reflections	843,512	209,617	113,946	641,724	118,218
$R_{\text{work}} / R_{\text{free}}$	0.20 (0.24) / 0.24 (0.29)	0.21 (0.31) / 0.25 (0.39)	0.18 (0.22) / 0.22 (0.28)	0.19 (0.26) / 0.23 (0.31)	0.21 (0.32) / 0.26 (0.39)
No. atoms	14,526	3693	7075	3805	3478
Protein	13,412	3356	6724	3460	3406
Ligand/ion (SO ₄)	35			50	10
Water	1079	337	351	295	62
B-factors (Å ²)	47	38	28	45	55
Protein	47	37	27	44	55
Ligand/ion	56			75	66
Water	43	42	32	49	49
R.m.s. deviations					
Bond lengths (Å)	0.008	0.01	0.005	0.008	0.003
Bond angles (°)	1.01	1.28	0.91	0.98	0.63

One crystal was used for each structure

*Values in parentheses are for highest-resolution shell.

b. Cryo-EM data collection and refinement statistics

	vFP16.02-DS-SOSIP-VRC03-PGT122 EMD-7460 6CDI	vFP20.01-DS-SOSIP-VRC03-PGT122 EMD-7459 6CDE	vFP1.01-DS-SOSIP EMD-8420	vFP5.01-DS-SOSIP EMD-8421, EMD-8422
Data collection and processing				
Magnification	22500	130000	22500	22500
Voltage (kV)	300	300	300	300
Electron exposure (e ⁻ /Å ²)	67.18	70.70	67.39	68.58
Defocus range (μm)	~ -1.0 - -4.0	~ -2.0 - -3.0	~ -1.8 - -4.0	~ -1.0 - -3.5
Pixel size (Å)	1.07	1.06	1.07	1.07
Symmetry imposed	C3	C3	C3	C1
Initial particle images (no.)	206112	108962	53263	45231
Final particle images (no.)	57278	48248	14931	7383, 41278
Map resolution (Å)	3.6	3.8	8.6	14.7, 19.6
FSC threshold	0.143	0.143	0.143	0.143
Map resolution range (Å)	3.4-8.9	3.4-8.7		
Refinement				
Initial model used (PDB code)	5FYL, 3SE8, 6CDO	5FYL, 3SE8, 6CDP		
Model resolution (Å)	3.7	3.9		
FSC threshold	0.5	0.5		
Model resolution range (Å)	10-3.6	10-3.4		
Map sharpening B factor (Å ²)	-68.00	-69.47		
Model composition				
Non-hydrogen atoms	33165	33057		
Protein residues	3849	3852		
<i>B</i> factors (Å ²)				
Protein	103.84	97.66		
R.r.m.s. deviations				
Bond lengths (Å)	0.008	0.007		
Bond angles (°)	1.02	0.960		
Validation				
MolProbity score	1.69	1.65		
Clashscore	7.62	5.15		
Poor rotamers (%)	0.18	0		
Ramachandran plot				
Favored (%)	93.84	94.47		
Allowed (%)	6.16	5.53		
Disallowed (%)	0	0		

Supplementary Table 5. Impact of alanine and glycine mutations at different FP residue positions on binding of FP-directed antibodies.

a

	vFP1.01	vFP1.02	vFP2.01	vFP3.01	vFP4.01	vFP5.01	vFP6.01	vFP7.01	vFP7.02	vFP7.03	vFP7.04	vFP7.05	vFP16.02	vFP20.01	VRC34.01
512	1.00	1.00	1.00	1.00	1.00	1.00	1.00	1.00	1.00	1.00	1.00	1.00	1.00	1.00	1.00
513	0.93	0.97	0.69	0.70	0.44	0.59	0.83	0.90	0.97	1.02	1.04	1.02	1.01	0.99	0.05
514	0.24	0.21	0.06	0.04	0.01	0.41	0.72	0.08	0.10	0.04	0.09	0.09	0.66	0.48	0.72
515	0.44	0.44	0.10	0.04	0.05	0.07	0.47	0.25	0.32	0.27	0.29	0.23	0.69	0.66	0.03
516	1.03	1.07	1.01	1.05	0.75	0.56	0.78	0.99	0.99	0.99	1.02	1.00	0.98	0.99	0.01
517	1.00	1.00	1.00	1.00	1.00	1.00	1.00	1.00	1.00	1.00	1.00	1.00	1.00	1.00	1.00
518	0.96	1.06	1.03	1.00	1.02	0.92	0.39	1.01	1.03	1.06	1.02	1.06	1.03	1.02	0.73
519	0.93	1.03	0.98	1.02	1.03	0.14	0.30	0.98	1.02	1.04	1.02	1.03	1.03	1.01	0.80
520	0.99	1.06	1.01	1.07	1.05	1.01	1.01	1.03	1.03	1.05	1.01	1.04	1.05	1.05	1.02
521	0.98	1.08	1.02	1.09	1.01	0.99	1.02	1.03	1.02	1.02	1.02	1.00	1.00	1.00	0.85

< 0.25 0.25 - 0.50 0.50 - 0.75 > 0.75

Binding of indicated antibodies to alanine mutants normalized to binding to the wild-type FP sequence. Experiments were performed in triplicate (n=3 independent experiments).

b

	vFP1.01	vFP1.02	vFP2.01	vFP3.01	vFP4.01	vFP5.01	vFP6.01	vFP7.01	vFP7.02	vFP7.03	vFP7.04	vFP7.05	vFP16.02	vFP20.01	VRC34.01
512	0.98	1.03	0.85	1.09	0.85	0.91	0.60	0.81	0.94	0.88	0.98	0.96	1.00	0.97	0.52
513	0.12	0.09	0.06	0.03	0.04	0.43	0.59	0.13	0.14	0.17	0.30	0.27	0.51	0.34	0.00
514	1.00	1.00	1.00	1.00	1.00	1.00	1.00	1.00	1.00	1.00	1.00	1.00	1.00	1.00	1.00
515	0.05	0.03	0.02	0.02	0.01	0.01	0.12	0.04	0.01	0.01	0.01	0.01	0.03	0.03	0.00
516	1.00	1.00	1.00	1.00	1.00	1.00	1.00	1.00	1.00	1.00	1.00	1.00	1.00	1.00	1.00
517	0.83	0.96	0.93	0.93	0.96	0.86	0.93	0.94	0.92	0.94	0.97	0.94	0.97	0.98	0.75
518	0.98	1.02	0.96	0.86	1.01	0.71	0.10	0.95	0.98	1.00	0.98	0.99	1.02	1.00	0.49
519	0.95	0.97	0.84	0.95	0.88	0.09	0.39	0.87	0.92	0.90	0.89	0.90	0.92	0.91	0.49
520	0.99	1.06	0.97	1.09	1.03	1.07	0.95	0.97	0.99	1.00	0.98	1.00	1.01	1.00	1.01
521	1.00	1.00	1.00	1.00	1.00	1.00	1.00	1.00	1.00	1.00	1.00	1.00	1.00	1.00	1.00

< 0.25 0.25 - 0.50 0.50 - 0.75 > 0.75

Binding of indicated antibodies to glycine mutants normalized to binding to the wild-type sequence. Experiments were performed in triplicate (n=3 independent experiments).

Supplementary Table 6. Prevalence of FP residue 512-519 by clades.

Clades A/ACD/AD		Clade AC		Clade AE		Clade AG		Clade B		Clades C/BC		Clades D/CD		Clade G	
Residue 512-519	Count														
AVGIGAVF	19	AVGIGAVF	3	AVGIGAMI	18	AVGLGAVF	8	AVGIGAVF	8	AVGIGAVF	28	AIGLGAMF	6	AVGMGAVL	2
AVGLGAVF	3	AVGLGAVF	2	AVGIGTMI	2	AVVGLGAVF	2	AVGTIGAMF	8	AVGLGAVF	10	AIGLGALF	4	EVTLGALF	1
AVTMGAVF	2			AVTIGAMI	1	AVGMGALI	1	AVGIGALF	5	AVGLGAVL	4	AIGLGAVF	3	AVGLGAVI	1
AVGFGAFF	2			AVGIGIMI	1	AVGMGALF	1	AVGIGAMF	3	AVGIGAVL	4	AIGMGALF	1	AVGLGAFL	1
AVVELGAVF	1			AVGIGALL	1	AVGLGALF	1	AVGTLGAMF	2	AVGIGAMF	4			AIGMGAVL	1
AVGMGAVF	1					AVGLGAFF	1	AVGLGAMF	2	AALGAVF	3			AIGLGTVL	1
AVGMAAVF	1					AIGMGAVF	1	TVGIGALF	1	AVGMGAVF	2				
AVGMAALF	1					AALGAVF	1	DLGLGALF	1	AVGIGAVI	2				
AIGMGAVF	1							AVTLGAVF	1	AVGIGALF	2				
AIGLGAMF	1							AVTLGAMF	1	TVGIGAVF	1				
								AVGMLGAMF	1	AVVGLGAVF	1				
								AVGLGAVF	1	AVGVGAVM	1				
								AVGLGALF	1	AVGTIGAMF	1				
								AVGIVGAMF	1	AVGLGAVI	1				
								AVGIGAVL	1	AVGLGAMI	1				
								AMGIGAMF	1	AVGLGAMF	1				
								AIGIGAVF	1	AVGGIGAVF	1				
								AALGALF	1	AVGGFGAMI	1				
								AAIGALF	1	AALGALF	1				
										AAGIGAVI	1				

Supplementary Table 7. Association of FP-proximal N-glycan sequons (N88, N241, N448, and N611) and neutralization based on the 208-isolate panel.

	vFP1.01	vFP7.04	vFP7.05	vFP16.02	vFP20.01	VRC34.01
88	1	1	1	1	1	0.7037
241	0.0122	0.0233	0.0122	0.9382	0.7846	0.7424
448	1	1	1	0.5804	0.6812	0.0327
611	0.4714	0.5504	0.4714	0.3986	0.9479	0.7037

Values displayed are P-values from the two-tailed Fisher's exact test and were corrected for multiple testing using Hohm metric. Statistically significant adjusted P-values are highlighted in red and corresponding contingency tables shown below. n=208 HIV-1 strains.

vFP1.01 - 241

	Resistant	Sensitive
Glycan	190	16
Non-glycan	1	1

vFP7.04 - 241

	Resistant	Sensitive
Glycan	183	16
Non-glycan	5	4

vFP7.05 - 241

	Resistant	Sensitive
Glycan	186	13
Non-glycan	5	4

vFP34.01 - 448

	Resistant	Sensitive
Glycan	94	86
Non-glycan	7	21

Supplementary Table 8. vFP antibody neutralization statistics from the 208-virus isolate panel.

IC ₅₀ <50 µg/ml	1868-vFP1.01	1868-vFP5.01	2586-vFP7.04	2586-vFP7.05	2712-vFP16.02	2716-vFP20.01	N123-VRC34.01
Neutralization breadth on 208 virus panel	8.17%	0.96%	9.62%	8.17%	31.3%	27.4%	51.4%
Neutralization breadth on global virus panel	8.33%	0%	8.33%	16.7%	41.7%	41.7%	75.0%
Neutralization breadth against neutralization-resistant isolates	7.69%	0%	8.33%	8.33%	28.9%	25.0%	50.0%
Neutralization breadth on FP8-sequence viruses	20.7%	1.72%	22.4%	17.2%	72.4%	74.1%	94.8%

IC ₅₀ <100 µg/ml	1868-vFP1.01	1868-vFP5.01	2586-vFP7.04	2586-vFP7.05	2712-vFP16.02	2716-vFP20.01	N123-VRC34.01
Neutralization breadth on 208 virus panel	9.62%	1.92%	11.1%	8.65%	36.5%	32.2%	51.92%
Neutralization breadth on global virus panel	16.7%	0%	8.33%	16.7%	41.7%	50.0%	75.0%
Neutralization breadth neutralization-resistant isolates	7.69%	0%	10.3%	8.97%	34.0%	28.9%	50.6%
Neutralization breadth on FP8-sequence viruses	25.9%	3.45%	27.6%	19.0%	81.0%	82.8%	94.8%

IC ₅₀ <500 µg/ml	2712-vFP16.02
Neutralization breadth on 208 virus panel	46.6%
Neutralization breadth on global virus panel	66.7%
Neutralization breadth neutralization-resistant isolates	46.1%
Neutralization breadth on FP8-sequence viruses	96.6%

Neutralization breadth of FP targeting neutralizing antibodies evaluated based on different virus panels: a 208-isolate panel evaluated in this study; the global panel (deCamp et al. 2013 JV); the neutralization-resistant strains in the 208-isolate panel (154 strains that were not neutralized by antibodies 17b, 48d, F105, 447-52D and 3074); the 58 strains in the 208-isolate panel that have the identical N-terminal 8-mer of the FP as BG505. Breadth statistics for IC₅₀<50 µg/ml are shown at top, statistics for IC₅₀<100 µg/ml are shown in the middle, and statistics for IC₅₀<500 µg/ml are shown at bottom.